NANO LETTERS

2001
Vol. 1, No. 3
161−163

Natural Rolling of Zigzag Multiwalled Carbon Nanotubes on Graphite

K. Miura,* T. Takagi, S. Kamiya, T. Sahashi, and M. Yamauchi

Department of Physics, Aichi University of Education, Hirosawa 1, Igaya-cho, Kariya 448-8542, Japan

Received February 5, 2001 *(Revised Manuscript Received February 16, 2001)*

ABSTRACT

The chirality of a multiwalled carbon nanotube (MWNT) on graphite has been determined to be of a zigzag type using frictional force microscopy. The force per angstrom required to rotate the zigzag MWNTs in-plane on graphite has been estimated to be approximately 4pN. Natural rolling induced by a tip contact appears in commensurate contact with a graphite surface. The difference between natural rolling and rolling with stick-slip lateral behavior is discussed.

Recently, nanotubes have become promising as ideal materials for lubrication because of their shape, which applies to C_{60} and C_{70} fullerenes. Sliding and rolling behaviors of nanotubes, including fullerene molecules, depend strongly on their interactions with the substrate.[1−6] For example, single-walled carbon nanotubes (SWNTs) were bent on a KCl(001) surface but were aligned on graphite, resulting in a 3-fold symmetry.[6] This is the reason that six carbon rings of the nanotube pair with those at the basal graphite surface in the same manner as the stacking of graphite layers. In this case, the sliding of the SWNTs on graphite does not occur because the SWNTs form a bundle of self-assembled cables and a nanotube array in the bundle contacts with graphite. In contrast, the SWNTs on a KCl(001) surface slide easily, resulting in a shear stress of 3MPa. Falvo et al.[1,2] showed the stick-slip lateral force behavior for rolling of multiwalled carbon nanotubes (MWNTs). However, their stick-slip lateral forces are very large, and the reason for their occurrence is not clear.

In this paper, we report on the sliding and natural rolling without stick-slip lateral forces of MWNTs on graphite evaluated using frictional force microscopy (FFM). We present the chirality of the MWNTs using a high-resolution frictional force microscope. It is shown that the lateral forces required to continue rolling MWNTs are not needed.

The powder of MWNTs (CarboLex AP-Grade Nanotubes) was dissolved in ethylene chloride using an ultrasonic bath to agitate the solution. After being dispersed on highly oriented pyrolytic graphite (HOPG) surfaces, MWNTs were imaged under an argon atmosphere using FFM. The normal and torsional spring constants of the cantilever with a Si_3N_4 tip (Microcantilever (OMCL-RC800PSA), Olympus Optical Co., Ltd.) were 0.05 N/m (experimentally estimated value) and 170.5 N/m (calculated value), respectively.

The FFM image of a MWNT on graphite is shown in Figure 1. Many MWNTs on graphite were aligned, resulting in a 3-fold symmetry, in a manner similar to SWNTs. The enlarged images of local area A in the graphite substrate and local area B in the MWNT are shown in the bottom part of Figure 1. The enlarged image of local area A exhibits a one-dimensional stick-slip motion, which shows that the scanning direction of a tip is identical with the $[12\bar{3}0]$ direction of the graphite substrate.[7,8] Also, it is noted that the enlarged image of local area B exhibits the same image as that of local area A. It is of interest to note that the angle between the axial direction of the nanotube and the $[12\bar{3}0]$ direction of the graphite substrate is 30°. This reveals that the chirality of this MWNT is a zigzag type. Assuming that the interaction between the MWNT and graphite relies on the outer graphene sheet of the MWNT, it is possible that the MWNT stacks on the graphite substrate in the same manner as the stacking (AB stacking) of graphite layers. This assumption is consistent with those of other cases such as C_{60} molecules on graphite,[5] SWNTs on graphite[6] and a graphite flake on graphite.[8] Most of the specimens observed in this experiment consisted of a zigzag MWNT.

Figure 2 shows the FFM image from the zigzag MWNT on graphite. First, a tip approaches the MWNT from the right and then comes into contact with it. The MWNT begins to rotate around a pivot point P out of commensurate contact (R_1). After rotating about 14°, the MWNT begins to rotate around a pivot point P′ (different from the pivot point P) out of commensurate contact (R_2). Furthermore, the MWNT begins to rotate around the pivot point P′ in commensurate contact (R_3). The vibration behavior shown in R_3 of Figure

* Corresponding author. E-mail: kmiura@auecc.aichi-edu.ac.jp

10.1021/nl015513y CCC: $20.00
Published on Web 03/14/2001

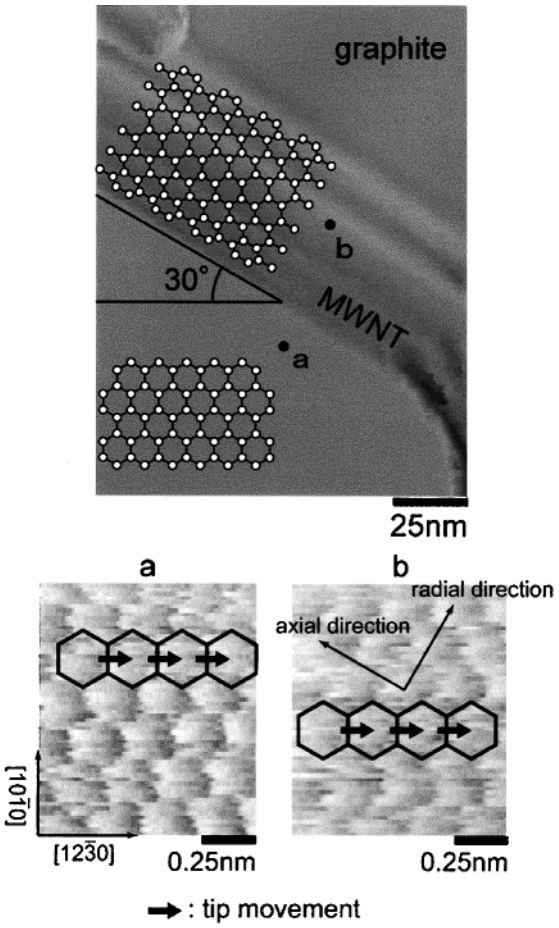

Figure 1. FFM image of the MWNT on the graphite surface. The enlarged images of local area A in the graphite substrate and local area B in the MWNT are shown at the bottom of the figure. The enlarged image of local area A exhibits a one-dimensional stick-slip motion, which shows that the scanning direction of a tip is identical with the [12$\bar{3}$0] direction of the graphite substrate. Also, it is noted that the enlarged image local area B exhibits is the same as that of local area A.

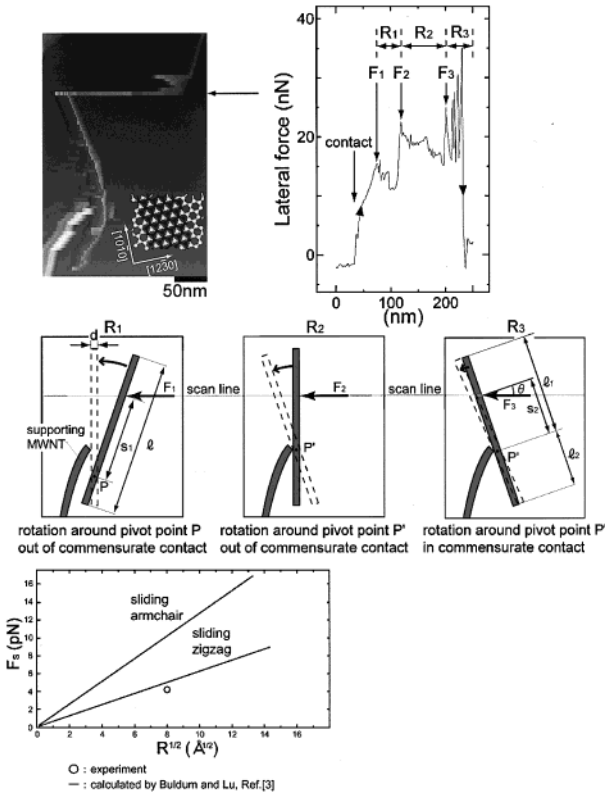

Figure 2. FFM image from the zigzag MWNT on graphite. The line profile (indicated by an arrow) is depicted on the right side of the figure. First, a tip approaches the MWNT from the right and then comes into contact with it. The MWNT begins to rotate around the pivot point P out of commensurate contact (R_1). After rotating about 14°, the MWNT begins to rotate around the pivot point P′ (different from pivot point P) out of commensurate contact (R_2). Furthermore, the MWNT begins to rotate around the pivot point P′ in commensurate contact (R_3). The bottom figure shows the forces (solid lines: Buldum and Lu, ref 3) per angstrom needed to slide the armchair and zigzag nanotubes and one (circle) estimated from experimental data.

2 is probably due to fluctuations in a supporting MWNT building up the pivot point P′. Thus, this in-plane rotation of the MWNT consists of both rotations out of commensurate and in commensurate contacts. It is noted that the force needed to begin rotating in commensurate contact is larger than that out of commensurate contact. Now, assuming that the shear stress σ between the MWNT and graphite is constant around the pivot point P′, the force per unit length required to rotate the MWNT, F_l is given as follows:

$$Fs_2 = \int_0^{l_1} \sigma l dl + \int_0^{l_2} \sigma l dl \qquad (1)$$

$$F_l = \sigma d = \frac{2Fs_2}{l_1^2 + l_2^2} \qquad l = l_1 + l_2 \qquad (2)$$

where d, s_2, and l are the contact width between the MWNT and graphite, the distance between the push point and the pivot point P′, and the length of the MWNT, respectively. In commensurate contact, F_l is estimated to be approximately 4 pN/Å using $F = 25$ nN ($F_3 \times \cos 17°$), $s_2 = 189$ nm, $l = 600$ nm, and $l_1 = 433$ nm, where the radius of this MWNT is 6.5 nm. This value is in excellent agreement with that of theoretical calculation for a zigzag nanotube. Using $\sigma = 0.2$ GPa[5], d is estimated to be approximately 0.2 nm, which corresponds to the lattice constant of graphite. This estimation is consistent with the result of Hertel et al.[9] that the deformation of a MWNT is very small.

Figure 3 shows the FFM image for rolling of the zigzag MWNTs on graphite. The upper two figures, A and B, show the characteristics of natural rolling. Both cases show that the original position and the final position keep in parallel after rolling. First, a first peak (F) appears which exhibits the lateral force required to push the MWNT. Then, the energies for MWNTs A and B used to push MWNTs are estimated to be 9.6×10^{-17}J and 3.4×10^{-17}J from the first peak area, respectively. After being pushed, the MWNT rolls naturally without a driving force. After rolling about two revolutions, the MWNT loses kinetic energy and stops. The tip catches up with the MWNT and scans over the MWNT, which is denoted by S in Figure 3.[6] However, the lower part

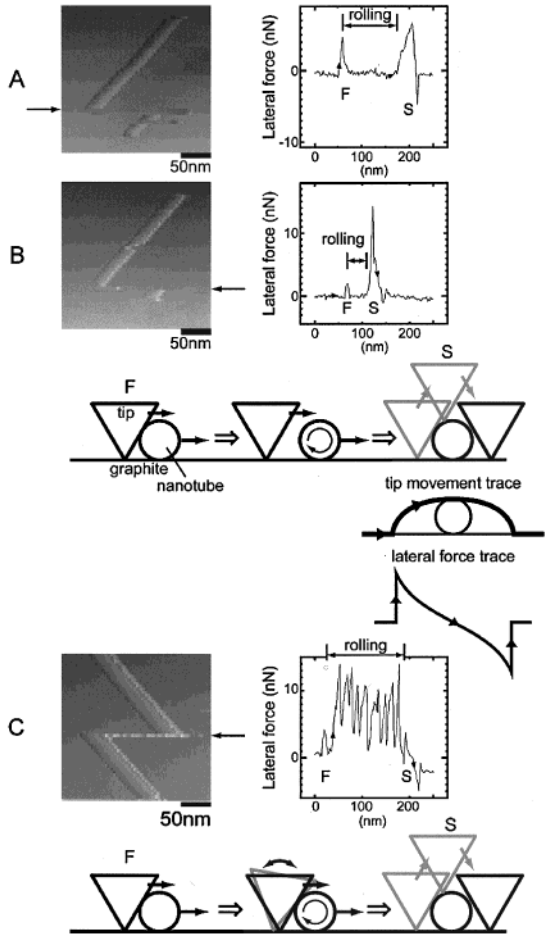

Figure 3. FFM image for rolling of the zigzag MWNTs on graphite. The line profile (indicated by an arrow) is depicted on the right side of the figure. The upper two (A and B) and the bottom (C) figures show the characteristics of natural rolling, and rolling with the several contacts with the tip during rolling, respectively.

C in Figure 3 exhibits stick-slip features. Even in this case, the MWNT translates in parallel. As reported by Falvo et al.,[1,2] the stick-slip features reveal that the tip again pushes the MWNT which, however, continues to roll. Even in this case, the rolling was about two revolutions. In the atomic force microscope (AFM) mode where a scan direction is parallel to the axis direction of a cantilever, the stick-slip features very often appear. Also, natural rolling only occurs under an argon atmosphere, although the stick-slip behaviors change little under the relative humidity (0−30%). Thus, rolling behaviors seem to depend on the relative humidity and the relative coordinate between the scanning direction of a tip and the axial direction of a MWNT, which controls the chance or probability where a tip again comes into contact with a MWNT during rolling. Furthermore, the fact that natural rolling occurs only under an argon atmosphere indicates that the adsorbed water molecules on graphite and/or a MWNT influence the distance of natural rolling; e.g., a MWNT is easy to lose kinetic energy and easily stops at a higher relative humidity. In the future, we plan to perform the experiments under an ultrahigh vacuum atmosphere in order to clarify the influence of adsorbed water layers.

Acknowledgment. We are grateful to S. Okita and M. Ishikawa for their technical assistance.

References

(1) Falvo, M. R.; Taylor, R. M., II; Helser, A.; Chi, V.; Brooks, F. P.; Washburn, S.; Superfine, S. *Nature* **1999**, *397*, 236.
(2) Falvo, M. R.; Steele, J.; Taylor, R. M., II; Superfine, R. *Phys. Rev. B.* **2000**, *62*, R10665.
(3) Buldum, A.; Lu, J. P. *Phys. Rev. Lett.* **1999**, *83*, 5050.
(4) Okita, S.; Ishikawa, M.; Miura, K. *Surf. Sci. Lett.* **1999**, *442*, L9590.
(5) Okita, S.; Miura, K. *Nano Lett.* **2001**, *1*, 101.
(6) Miura, K.; Ishikawa, M.; Kitanishi, R.; Yoshimura, M.; Ueda, K.; Tatsumi, Y.; Minami, N. *Appl. Phys. Lett.* **2001**, *78*, 832.
(7) Sasaki, N.; Kobayashi, K.; Tsukada, M. *Phys. Rev. B* **1996**, *54*, 2138.
(8) Miura, K., unpublished.
(9) Hertel, T.; Walkup, R. E.; Avouris, P. A. *Phys. Rev. B* **1998**, *58*, 13870.

NL015513Y